Inhibition of Macrophage Migration Inhibitory Factor or Its Receptor (CD74) Attenuates Growth and Invasion of DU-145 Prostate Cancer Cells[1]

Katherine L. Meyer-Siegler,[2]*† Kenneth A. Iczkowski,‡§ Lin Leng,¶ Richard Bucala,¶ and Pedro L. Vera*†

Macrophage migration inhibitory factor (MIF), a proinflammatory cytokine, is overexpressed in prostate cancer, but the mechanism by which MIF exerts effects on tumor cells remains undetermined. MIF interacts with its identified membrane receptor, CD74, in association with CD44, resulting in ERK 1/2 activation. Therefore, we hypothesized that increased expression or surface localization of CD74 and MIF overexpression by prostate cancer cells regulated tumor cell viability. Prostate cancer cell lines (LNCaP and DU-145) had increased MIF gene expression and protein levels compared with normal human prostate or benign prostate epithelial cells ($p < 0.01$). Although MIF, CD74, and CD44 variant 9 expression were increased in both androgen-dependent (LNCaP) and androgen-independent (DU-145) prostate cancer cells, cell surface of CD74 was only detected in androgen-independent (DU-145) prostate cancer cells. Therefore, treatments aimed at blocking CD74 and/or MIF (e.g., inhibition of MIF or CD74 expression by RNA interference or treatment with anti-MIF- or anti-CD74- neutralizing Abs or MIF-specific inhibitor, ISO-1) were only effective in androgen-independent prostate cancer cells (DU-145), resulting in decreased cell proliferation, MIF protein secretion, and invasion. In DU-145 xenografts, ISO-1 significantly decreased tumor volume and tumor angiogenesis. Our results showed greater cell surface CD74 in DU-145 prostate cancer cells that bind to MIF and, thus, mediate MIF-activated signal transduction. DU-145 prostate cancer cell growth and invasion required MIF activated signal transduction pathways that were not necessary for growth or viability of androgen-dependent prostate cells. Thus, blocking MIF either at the ligand (MIF) or receptor (CD74) may provide new, targeted specific therapies for androgen-independent prostate cancer. ***The Journal of Immunology,*** **2006, 177: 8730–8739.**

The inflammatory response is central to the functioning of the innate immune system. Alterations in inflammatory response control are characteristic of numerous chronic inflammatory pathologies, including cancer (1). Many cancers arise from sites of infection, chronic irritation, and inflammation, with the resulting tumor cells using some of the signaling molecules of the inflammatory response, such as cytokines, chemokines, and their receptors, which aid in tumor cell invasion, migration, and metastasis (2).

Recent data support the hypothesis that there is a link between chronic prostate inflammation and prostate cancer (3). Prostate cancer is the second most common malignancy in American men, with estimates projecting that >232,000 new cases were diagnosed in the United States in 2005. Epidemiological studies have determined an associated risk between prostate cancer in men with a prior history of certain sexually transmitted infections or prostatitis, suggesting that prostate inflammation may modulate prostate cancer growth (4–6).

Our research has focused on understanding the contribution of a unique proinflammatory cytokine, macrophage migration inhibitory factor (MIF)[3] and its cell surface receptor (CD74) to prostate cancer (7, 8). MIF is constitutively expressed in luminal epithelial cells, which are continuously exposed to environmental insult. In the epithelial cell, intracellular MIF stores may maintain cell inflammatory response by acting in cooperation with glucocorticoids to control both the set point and the magnitude of the response (9). Although MIF is essential for innate immune response, any shift toward MIF up-regulation increases the likelihood of chronic inflammatory disease and cancer outgrowth (10). Various inflammatory cytokines are implicated in maintaining tumor cell growth and viability. MIF is unusual in its contribution to the growth and survival of a developing neoplasm, first and foremost, because it is constitutively expressed and stored, preformed, in cells (9). Secondly, MIF is unique because it functions in many processes associated with tumor survival including cell division, angiogenesis, and suppression of host-tumor cell immune surveillance (11). The precise mechanisms of MIF in tumorigenesis are still being investigated. However, MIF suppresses the action of the tumor-suppressor gene p53, resulting in promotion of cell growth and inhibition of apoptosis (12, 13).

*The Bay Pines Veterans Affairs Healthcare System, Research and Development, Bay Pines, FL 33744; †University of South Florida, Department of Surgery, Tampa, FL 33612; ‡Malcom Randall Veterans Affairs Medical Center, Department of Pathology, Gainesville, FL 32608; §University of Florida College of Medicine, Department of Pathology, Immunology, and Laboratory Medicine, Gainesville, FL 32610; and ¶Yale University School of Medicine, New Haven, CT 06520

Received for publication June 7, 2006. Accepted for publication October 2, 2006.

The costs of publication of this article were defrayed in part by the payment of page charges. This article must therefore be hereby marked *advertisement* in accordance with 18 U.S.C. Section 1734 solely to indicate this fact.

[1] Supported by Veterans Affairs Merit Review Program (to K.L.M.-S. and P.L.V.), the Bay Pines Foundation (to K.L.M.-S. and P.L.V.), and National Institutes of Health (to R.B. and L.L.).

[2] Address correspondence and reprint requests to Dr. Katherine L. Meyer-Siegler, Bay Pines Veterans Affairs Health Care System, Research and Development (151), 10000 Bay Pines Boulevard, Bay Pines, FL 33744. E-mail address: Katherine.Siegler@med.va.gov

[3] Abbreviations used in this paper: MIF, macrophage inhibitory factor; CD44v9, CD44 variant 9; PrEC, human prostate epithelial cells; PVDF, polyvinylidene difluoride; RNAi, RNA interference; PCNA, proliferating cell nuclear Ag; p-ERK, phosphorylated ERK; pNA, *p*-nitroaniline.

0022-1767/06/$02.00

CD74, the MIF receptor, is a type II transmembrane protein that is part of the MHC (14). CD74 functions to regulate the loading of exogenously derived peptides onto MHC class II heterodimers (15). However, recent studies demonstrated that CD74 is transiently expressed on the cell surface in diverse cells including monocytes, B cells, fibroblasts, and urothelial cells, as well as the prostate (8, 16–18). The exact function of cell surface CD74 has not been determined. However, MIF binds to the extracellular domain of CD74 with high affinity, and such binding is required for MIF activation of ERK 1/2 MAPK cascade (19). In addition, we recently demonstrated that inflammation induced increases in MIF-CD74 interaction at sites of inflammation, suggesting a physiological role for MIF-CD74 binding early in the inflammatory response (17). A recent study by Starlets et al. (20) documents MIF-CD74 induction of signaling cascade that activates NF-κB and induces DNA synthesis and cell entry into the S phase as well as Bcl-x_L expression, suggesting that CD74 functions as a survival receptor.

The cytosolic domain of CD74 is very short and appears to lack intracellular signaling domains (20). Recent studies have identified recruitment of transmembrane CD44 as a potential accessory protein required for MIF-CD74 signal transduction (21, 22). In addition, we recently showed the formation of a molecular complex between MIF, CD74, and CD44 in HT-1376 bladder carcinoma cells (23). Prostate cancer loses expression of standard CD44 and overexpresses almost entirely variant forms, which arise from alternate splicing of exons 7–10 (24), thus suggesting that variant forms of CD44 (e.g., CD44 variant 9 (CD44v9)) may be involved in MIF-CD74-mediated signal transduction in prostate cancer.

Androgens are critical to the growth and differentiation of prostate epithelial cells (3). Removal of androgen normally results in apoptosis, but androgen-independent tumors have developed mechanisms that allow cells to survive the loss of androgen. Clinical prostate cancer progression may be the result of the regrowth of cells that adapted to the low-androgen environment and resumed proliferation. In vitro prostate cancer cell models showed that the regrowth of androgen-independent cells was associated with increased expression of cyclin D1, indicating that the emergence of androgen independence is associated with a release from cell cycle arrest (25).

Based on our previous studies, our model shows that MIF-CD74-CD44 interaction is required for normal prostate inflammatory responses. Our laboratory was first in describing the association between increased MIF expression in prostate tumor tissue, as well as the association between elevated serum MIF and prostate cancer (7). In prostate cancer, cell surface association of MIF and CD74 may play an essential role in cell survival. Thus, our working hypothesis is that the blockade of MIF or its recently identified receptor (CD74) will impede or reduce prostate cancer cell growth. In this study, we demonstrated cell surface localization of the MIF receptor (CD74) in aggressive, androgen-independent (DU-145) prostate cancer cells and that biologically active MIF and/or the MIF receptor (CD74) are necessary for the growth and invasion of these cells.

Materials and Methods

Cell culture

Normal human prostate epithelial cells (PrEC) were obtained from Cambrex and cultured exclusively in prostate epithelial cell growth medium. Human prostate cancer cell lines (LNCaP, DU-145) were obtained from the American Type Culture Collection (ATCC). Benign prostate epithelial cells (BPH-1) were obtained from Dr. Simon Hayward (Vanderbilt University, Nashville, TN). These cells were routinely cultured in RPMI 1640 with Glutamax supplemented with 10% FBS (standard growth medium). All cells were routinely grown without antibiotics in a 5% CO_2, 37°C humidified incubator. Cell proliferation was evaluated using a WST-1 (4-[3-(4-iodophenyl)-2-(4-nitrophenyl)-2*H*-5-tetrazolio]-1,3-benzene disulfonate) to formazan assay (Chemicon International). WST-1 reagent was added to the culture medium (1/10 dilution), and absorbance was measured at 450 nm following incubation at 37°C for 3 h.

Cell lysis, Western blot, coimmunoprecipitation, and biotinylation of cell surface proteins

Cell lysates from $\sim 2 \times 10^7$ subconfluent cells were prepared using lysis buffer (50 mM Tris-HCl (pH 7.5), 150 mM NaCl with 1% Triton X-100, 0.1% SDS, and 0.25% sodium deoxycholate) with the addition of general protease inhibitors (Sigma-Aldrich), and protein concentrations were determined using the MicroBCA protocol (Pierce). Cell lysate protein (15 μg) was separated by 4–12% Bis-Tris SDS-PAGE (Invitrogen Life Technologies) and transferred as described previously (23). Blots were blocked in blocking buffer (1% BSA, 10 mM PBS (pH 7.5), and 0.05% Tween 20) for 1 h at 37°C and incubated overnight with primary Ab (1/1000 dilution) at 4°C, followed by incubation with appropriate biotinylated secondary Ab and avidin-HRP (Vectastain ABC; Vector Laboratories). Individual protein bands were visualized by ECL (Pierce), and band intensities quantified using Kodak Image Station (Kodak). The following Abs were used in Western blotting: affinity purified goat anti-human MIF polyclonal Ab was obtained from R&D Systems (AF-289-PB); goat polyclonal anti-human CD74 was obtained from Santa Cruz Biotechnology (sc-5438); and monoclonal anti-human CD44v9 was used undiluted from hybridoma cell culture medium (HB-258; ATCC). CD44v9 amounts were examined rather than standard CD44 because variant forms are overexpressed in prostate cancer cell lines, and this variant represents the longest exon product within this sequence (24). β-Actin immunostaining of stripped blots was used as a loading control. MIF-interacting proteins were detected by coimmunoprecipitation using immobilized MIF polyclonal Ab (50 μg) conjugated to agarose beads (Seize X protein G-agarose; Pierce). Cell lysate (250 μl) was diluted 1/1 with PBS and incubated with Ab-coupled gel overnight at 4°C with end-over-end mixing. The resin was then washed with PBS until no protein was detected by A_{280} in the flow through and the bound proteins eluted with 200 μl of 100 mM glycine (pH 2.5). The pH of the eluted fractions was neutralized by the addition of 1 M Tris (pH 9.5), 1/20 dilution. The coimmunoprecipitated samples were separated by SDS-PAGE, and CD74 or CD44v9 immunostaining bands were detected as described for Western blotting.

To biotinylate cell surface proteins, BPH-1, LNCaP, or DU-145 cells (3×10^7) were plated into T75 culture flasks and grown for 48 h in standard growth medium. Adherent cells were washed three times with ice-cold PBS (pH 8.0) and 3 ml of 10 mM sulfosuccinimidyl-6-(biotin-amido)hexanoate (Pierce) PBS (pH 8.0) added to flask. The reaction mixture was incubated for 2 h at 4°C (to reduce active internalization of biotin reagent), and then cells were gently scraped from the flask surface. Labeled cells were collected by centrifugation, and the resulting pellet was washed three times with 15 ml of ice-cold 100 mM glycine in PBS (pH 8.0). Cell lysis buffer with general protease inhibitor mixture was added and biotinylated proteins were purified from lysates using avidin-agarose (Sigma-Aldrich). The resulting avidin-purified biotinylated proteins were concentrated 10-fold using a rotary vacuum evaporator (Brinkman Instruments) and 15 μl of the concentrated purified proteins processed for SDS-PAGE were transferred to a polyvinylidene difluoride (PVDF) membrane as described above. Biotinylated proteins were detected using HRP-conjugated streptavidin and chemiluminescent substrate. mAbs were used in the immunoprecipitation of biotinylated proteins as follows: LN2 specific for the carboxy terminus of human CD74 was obtained from Santa Cruz Biotechnology (sc-6262), mAb specific for human MIF was obtained from R&D Systems (MAB289), and CD44v9 mAb (HB-258; ATCC) was purified from cell culture supernatant by protein G-agarose. Avidin-purified biotinylated proteins were precleared with 10% weight-to-volume ratio protein G-agarose slurry (Kirkegaard & Perry Laboratories). Biotinylated MIF, CD74, or CD44v9 were immunoprecipitated with 5 μg of respective Ab overnight at 4°C with rocking, followed by incubation with 10% protein G-agarose slurry for 2 h with rocking. Immune complexes were dissociated with 40 μl of 2× sample buffer (Invitrogen Life Technologies) and incubated at 100°C for 5 min. The eluates were removed, dithiothreitol was added, and samples were incubated at 100°C for 5 min before loading on SDS-PAGE gels as described for Western blotting. Biotinylated proteins were detected using HRP-conjugated streptavidin and chemiluminescent substrate (Pierce).

MIF *genotype*

Two *MIF*-promoter polymorphisms (−173 G to C transition and seven copies of the −794 CATT repeat) are associated with increased MIF expression and are strongly associated with protein production. These genotypes were determined in BPH-1, LNCaP, and DU-145 cells by isolating genomic DNA from 1×10^6 subconfluent using DNAzol (Invitrogen Life Technologies) and genotyping as described previously (26).

Tautomerase activity

For the purposes of detecting MIF activity in biological samples, we developed a modified tautomerase assay using human recombinant MIF produced as described previously as a standard native sequence (27). DU-145, LNCaP, and BPH-1 cells were cultured with standard growth medium in T75 flasks until 80% confluent. Cells were lysed using lysis buffer, and spent culture medium was collected; 4 mM L-3,4-dihydroxyphenylalanine methyl ester (Sigma-Aldrich) and 20 mM sodium *m*-periodate (Sigma-Aldrich) were freshly prepared in water. Samples to be tested (60 μl, diluted if necessary in 10 mM sodium phosphate/1 mM EDTA (pH 6.2)) were pipetted into a standard polystyrene ELISA plate. Two hundred microliters of substrate (L-dopachrome methyl ester), prepared by mixing 72 μl of periodate stock with 108 μl of dihydroxyphenylalanine in 1620 μl of 10 mM sodium phosphate/1 mM EDTA (pH 6.2), was added. The samples were mixed and the change of A_{475} due to dopachrome tautomerization was monitored for 2 min. Inhibition of MIF tautomerase activity was determined by addition of MIF antagonist (*S*,*R*)-3-(4-hydroxyphenyl)-4,5-dihydro-5-isoxazole acetic acid methyl ester (ISO-1, final concentrations from 0.1 to 100 μM) to cell lysates just before measurement of tautomerase activity (28). Data are expressed as change of A_{475} nm per second per milligram of total protein. To assess the effects of blocking MIF activity on cell proliferation, DU-145, LNCaP, and BPH-1 cells (1×10^5 per well; 96-well plate) were plated in RPMI 1640 with 10% FBS for 6 h, and then treated with ISO-1 (final concentrations from 0.1 to 20 μM) for 18 h. Control cultures were treated with 0.1% DMSO. Cell proliferation was assessed by WST-1 assay, and data were expressed as percentage of control.

Antibody treatment

DU-145, LNCaP, and BPH-1 cells (1×10^4 per well of 96-well plate) were plated in RPMI 1640 with 10% FBS for 6 h, and then treated with either MIF (AF-289-PB) or CD74 Ab (sc-5438) goat polyclonal Ab at a final concentration of 2 μg/ml for 72 h total with cell proliferation and apoptosis assessed at 24 h intervals. Control cell cultures were treated with nonspecific goat IgG (Vector Laboratories). Cell proliferation was evaluated using the WST-1 to formazan assay (Chemicon International) as described above.

RNA interference (RNAi)

BPH-1, LNCaP, or DU-145 cells were seeded in 6-well tissue culture plates (2×10^5 cells per well) and grown in standard growth medium at 37°C in a CO_2 incubator for 48 h, at which time they were ~80% confluent. Cells were transfected with MIF RNAi (sc-37137; Santa Cruz Biotechnology) or CD74 RNAi (sc-35023; Santa Cruz Biotechnology) using LipofectAMINE 2000 transfection reagent (Invitrogen Life Technologies) following the manufacturer's protocol. Following incubation at 37°C for 7 h in a CO_2 incubator, 1 ml of RPMI 1640 with Glutamax and 20% FBS without antibiotics was added and growth continued for 18 h. The transfection medium was then removed and replaced with normal growth medium. Every 24 h for the next 72 h, cell proliferation was assayed using WST-1 dye metabolism as described above. Six wells were collected every 24 h; half the wells were processed for total protein, and the other half were processed for total RNA. Control wells were treated with scramble RNAi (sc-37007).

Apoptosis assays

Apoptosis was assessed by caspase-3 activity and DNA laddering. For assessment of caspase-3 activity, 2×10^6 cells were plated into 12-well culture dishes 6 h before RNAi treatment. After 48 h, cells were dislodged mechanically and washed twice in PBS. Caspase-3 activity was assessed using the BD ApoAlert caspase-3 colorimetric assay kit (BD Biosciences) as described by the manufacturer. *p*-Nitroaniline (pNA) was measured using a plate reader (Bio-Tek Instruments) at 405 nm. z-DEVD-fmk, a specific inhibitor of caspase-3, was used to confirm assay specificity. For DNA-laddering analysis, 48 h Ab-treated cells were harvested from cell wells and cell culture medium. The resulting cell pellet was washed in PBS, and genomic DNA was isolated by the direct addition of DNAzol (Invitrogen Life Technologies). DNA (2 μg) was resolved on 1.5% agarose gels with a 10- to 0.5-kb DNA marker for fragment size reference (Kilobase DNA marker; GE Healthcare).

Matrigel invasion

Matrigel invasion assay was conducted in 24-well Transwell culture plates containing microporous (3.0 μm) membranes coated with Matrigel (Costar). In brief, DU-145, LNCaP, or BPH-1 cells (3×10^4 cells/well) were added to the upper chamber containing basal medium (RPMI 1640 with 0.1% BSA) with appropriate Ab (2 μg/ml), and transmigration toward a serum gradient (70% standard growth medium, 20% conditioned medium, and 10% FBS with appropriate Ab at 2 μg/ml) in the lower chamber continued for 18 h. Following the incubation period, the nonmigrating cells were removed from the upper chamber using a cotton swab, and the adherent cells on the lower surface of the insert were stained with toluidine blue, and total invading cells were counted in nine representative fields at ×400 magnification. The data were expressed as average number of cells per treatment per ×400 field ± SE and were analyzed by ANOVA; $p < 0.05$ was considered statistically significant.

Real-time PCR

Total RNA was isolated from RNAi-treated DU-145 cells and reverse transcribed as described previously (23). Real-time PCR determination of MIF, CD74, and CD44v9 cDNA amounts were determined using a SYBR green reagent and the appropriate PCR primers (MIF-PPH00548A, CD74-PPH05587A, and CD44v9-PPH00114A; SuperArray) normalized to an 18S rRNA internal standard (PPH05666A; SuperArray). Temperature cycling and real-time fluorescence measurements were performed using an Opticon Monitor system (MJ Research). The PCR conditions were as follows: initial incubation at 95°C for 15 min, followed by 40 cycles of 95°C for 30 s, 55°C for 30 s, and 72°C for 30 s with incubation at 85°C for 15 s before the plate was read. The relative quantification of gene expression was performed using the comparative C_T ($\Delta\Delta C_T$) method following initial validation experiments that verified that the amplification efficiencies of MIF, CD74, CD44v9, and 18S rRNA were approximately equal as determined by ΔC_T with serial dilution of the control template. Plots of ΔC_T vs cDNA concentration were fit using least-squares regression analysis with the resulting slopes close to zero (MIF = −0.072, CD74 = 0.070, and CD44v9 = 0.069) indicating that relative changes in gene expression could be determined by $\Delta\Delta C_T$ (29). The $\Delta\Delta C_T$ was calculated as the difference between the normalized C_T values (ΔC_T) of the treatment and the control samples: $\Delta\Delta C_T = \Delta C_{T\ \text{treatment}} - \Delta C_{T\ \text{control}}$. $\Delta\Delta C_T$ was converted to fold change by the following formula: fold change $= 2^{-\Delta\Delta C_T}$ (29).

ERK 1/2 activation

The effect of MIF or CD74 RNAi treatment on ERK 1/2 activation was examined by Western blotting with Abs specific for phosphorylated (activated) ERK 1/2 (AF-1018; R&D Systems). BPH-1, LNCaP, and DU-145 cells were treated with RNAi for 72 h, and Western blotting was performed as described above. The membrane was then stripped and reprobed with ERK 1/2 Ab specific for total ERK 1/2 to normalize for differences in protein loading (AF-1576; R&D Systems).

Gene expression array analysis

A GEArray Q series human cancer (HS-044) and G-protein (HS-025) array kits were obtained from SuperArray. Included in these arrays are TNF-α and IL-1β, which are genes associated with downstream activation by MIF (30). DU-145 cells were cultured and treated as described above for RNAi experiments. The cells were pooled from three separate experiments (2×10^5 cells per experiment) to decrease bias. After 72 h of RNAi treatment, cells were harvested, total RNA was isolated with TRIzol reagent (Invitrogen Life Technologies), and 5 μg of RNA was used as a template to generate biotin-16-dUTP-labeled cDNA probes (AmpoLabeling-LPR kit; SuperArray). The cDNA probes were denatured and hybridized to membrane at 60°C overnight, and the resulting image was analyzed using the GEArray analyzer program (SuperArray). In brief, spot intensity was normalized by subtraction of the background of the average intensity value of three blank spots. The averages of two ribosomal protein RPL13A spots were used as positive controls and set as baseline values with which the signal intensity of other spots was compared. The array data represents mean fold variation of pooled samples from two separate arrays. RNAi-induced differences in gene expression were considered as present when the mean fold change was ≥2.0. Data are expressed as increased or decreased compared with controls (i.e., DU-145 cells treated with scramble RNAi, control vs DU-145 cells treated with message-specific RNAi).

ISO-1 treatment of DU-145 xenografts

All animal experiments were done according to regulations approved by the Institutional Animal Care and Use Committee. In brief, 250 μl of DU-145 human prostate carcinoma cells (5×10^6 cells) in Matrigel (BD Biosciences) were inoculated s.c. into the flank of 5- to 6-wk-old nude male mice weighing 20 to 25 g (Harlan). Immediately following cell implantation, ISO-1 (at 20 mg/kg) or vehicle (5% DMSO) was injected i.p. Mice were injected twice a week (Tuesday and Friday) for a total of 10 doses per mouse ($n = 4$ mice per group). The tumor size was measured by calipers and recorded weekly for a period of 35 days. Tumor volume was estimated using the formula: $(\text{width})^2 \times \text{length}/2$, measured in millimeters. At the end of the treatment, the mice were sacrificed and the tumors were removed, weighed, and processed for immunohistochemistry and protein. Serum was collected for human MIF ELISA determination using our previously described assay protocol (8). Tumor size and MIF amounts, represented as mean $\pm$ SE, were analyzed by Student's t test. Values of $p < 0.05$ were considered as statistically significant.

Immunohistochemical staining xenograft tumors

Excised tumors were fixed in 4% buffered formaldehyde. Immunohistochemical staining was done as previously described (17). In brief, paraffin-embedded 4-μm tumor sections were overlaid with goat anti-proliferating cell nuclear Ag (PCNA) or rat anti-CD34 Ab (sc-9857 or sc-18917, respectively; Santa Cruz Biotechnology). Sections were incubated with appropriate biotinylated secondary Abs (Vector Laboratories) and visualized with streptavidin-biotin conjugated with HRP (Vector Laboratories). CD34 immunostained sections were counterstained with H&E, whereas PCNA sections were not. For quantitative analysis, stained nuclei (PCNA) or cells (CD34) were counted in 10 areas from all tumors at $\times 40$ total magnification. The results were averaged for each treatment and expressed as mean $\pm$ SE. Data were analyzed by ANOVA; $p < 0.05$ was considered as statistically significant.

Results

Increased MIF, CD44v9, and CD74 protein expression in prostate cancer cells. Cell surface expression of CD74 is found only in androgen-independent DU-145 cells

Western blot analyses showed that MIF, CD74 (MIF receptor), and CD44v9 (signaling component of the MIF membrane receptor complex) amounts were increased in prostate cancer cell lines compared with benign prostate cells (Fig. 1, *A* and *B*). Invasive androgen-independent cells (DU-145) synthesize more MIF, CD74, and CD44v9 than noninvasive CaP cells (LNCaP) or benign BPH-1 cells ($p < 0.001$, unpaired t test; Fig. 1, *A* and *B*). Moreover, determination of the *MIF* genotype in these cells showed that the increased protein expression seen in DU-145 cells was associated

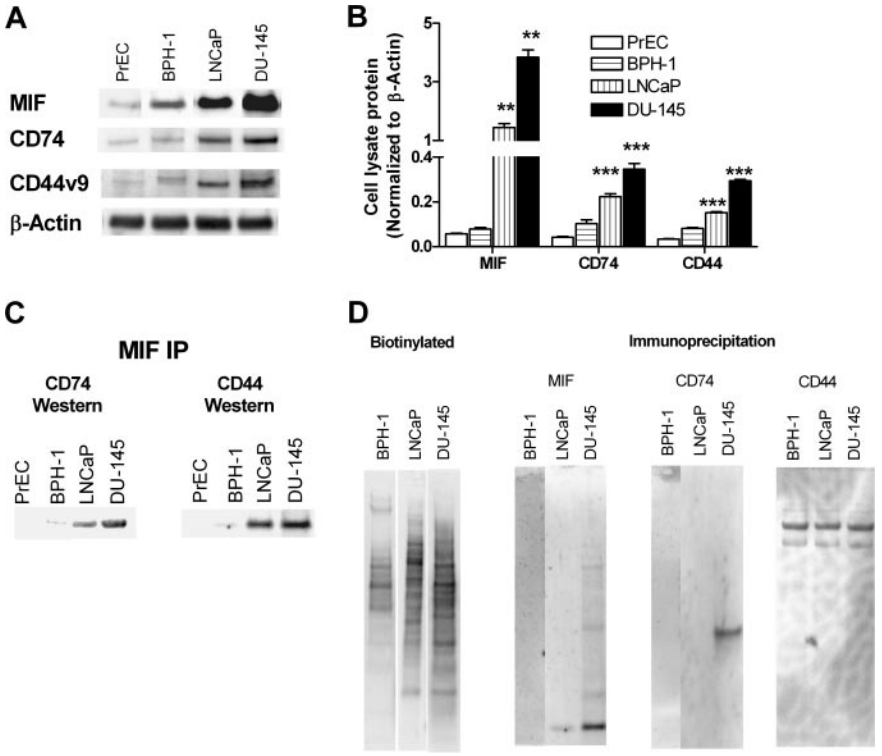

FIGURE 1. MIF signaling components in prostate epithelial cells. *A*, Representative Western blot bands. Cell lysates (10 μg of total protein) from 80% confluent cells grown under standard conditions were separated by SDS-PAGE under reducing conditions and transferred to PVDF membranes. Western blots were developed using anti-human MIF, anti-human CD74, or anti-human CD44v9 Abs. β-Actin was used as a loading control. Figures depict representative samples from duplicate experiments displayed as composites of multiple Western blots. *B*, Analysis of MIF signaling components in epithelial cells. Prostate cancer cell lines (LNCaP and DU-145) demonstrate increased protein content of all components of MIF signaling ($p < 0.001$) compared with benign prostate epithelial cells (PrEC and BPH-1). All band intensities were normalized to β-actin. Significant difference compared with PrEC is represented by asterisks as follows: **, $p < 0.01$; ***, $p < 0.001$. Values represent the mean $\pm$ SEM of duplicate measurements. Results are representative of duplicate experiments. *C*, Coimmunoprecipitation of CD74 and CD44v9 with MIF in prostate cancer cells. Cell lysates from 80% confluent cells (200 μg of total protein) were immunoprecipitated with MIF polyclonal Ab and the protein G-binding protein complexes were separated by SDS-PAGE followed by Western blotting using anti-CD74 or CD44v9 Abs. Figures depict representative samples from duplicate experiments displayed as composites of multiple Western blots. *D*, Cell surface expression of MIF and CD74 in prostate epithelial cells. Biotinylation: DU-145 cells express increased total cell surface proteins. BPH-1 and DU-145 cell surface proteins were labeled with biotin. Avidin-purified cell lysates were separated by SDS-PAGE, transferred to PVDF membranes, and total biotinylated protein was detected using HRP-labeled streptavidin. Immunoprecipitation: DU-145 express increased cell surface MIF and CD74 compared with BPH-1 cells. Avidin-purified biotinylated cell lysates were immunoprecipitated with monoclonal MIF, CD44v9, or monoclonal CD74 Ab. The resulting immunoprecipitate was separated by SDS-PAGE, transferred to PVDF membranes, and total biotinylated protein was detected using HRP-labeled streptavidin. Figures depict representative samples from duplicate experiments displayed as composites of multiple Western blots.

with the high-expression −173 G/C *MIF* polymorphism and the high-expression −794 6/7 CATT repeat polymorphism (25). The BPH-1 and LNCaP cells both contain the lower expressing G/G, 6/6 *MIF* polymorphisms.

CD74-MIF and CD44v9-MIF interactions in cell lysates as demonstrated by coimmunoprecipitation showed an increase in the amount of MIF interacting with CD74 and CD44v9 in prostate cancer cells (DU-145, LNCaP) when compared with benign prostate cells (PrEC, BPH-1; Fig. 1*C*).

To test the relationship between relative amounts of cell surface CD74, thus leading to MIF/CD44v9/CD74 interactions and prostate cancer aggressiveness, BPH-1, LNCaP, and DU-145 cell surface proteins were labeled with biotin, and avidin-purified biotinylated cell lysates were immunoprecipitated with MIF, CD44v9, or CD74 mAbs and detected using HRP-labeled streptavidin. Prostate cancer cells express greater cell surface protein amounts than BPH-1 cells (Fig. 1*D*). Examination of the particular proteins of interest (CD74, MIF CD44v9) showed that only DU-145 cells express cell surface CD74. In addition, DU-145 cells express a greater amount of cell surface MIF than LNCaP cells and cell surface MIF was not detected in BPH-1 cells (Fig. 1*D*). Because a small amount of cell surface MIF was detected in LNCaP cells, it is possible that these cells also expressed cell surface CD74 (thus binding MIF) albeit at a much lower amount and, thus, below the CD74 immunoprecipitation detection level. The possibility that MIF may bind to other cell surface proteins, however, cannot be ruled out at this point. Finally there was no difference in the cell surface amounts of CD44v9 expressed in BPH-1, LNCaP, or DU-145 cells (Fig. 1*D*). These results suggest that increased cell surface expression of CD74 allows greater binding of secreted MIF molecules by CD74 and, if this is the case, greater activation of CD74-mediated signaling pathways (e.g., ERK activation). Increased cell surface expression of CD74 in DU-145 cells compared with LNCaP and benign cells suggests that this mechanism may be associated with androgen-independent prostate cancer cell growth.

MIF-specific inhibitor (ISO-1) reduces MIF tautomerase activity and cell proliferation in DU-145 cells only

MIF is readily detectable within prostate cells in vitro and is actively secreted into the culture medium. However, it is not known whether intracellular and/or secreted MIF is biologically active. ISO-1 is a nontoxic inhibitor of MIF that binds to bioactive MIF at a catalytically active, tautomerase site within this cytokine (28). This is a useful target of MIF function, because the tautomerase activity can be measured by in vitro assay to determine the presence of bioactive MIF. MIF tautomerase activity was detected in cell lysates (Fig. 2*A*) and spent culture medium (Fig. 2*B*) from subconfluent BPH-1, LNCaP, and DU-145 cultures, indicating that MIF has biological activity both inside the cell and following secretion into the culture medium. In addition, intracellular MIF tautomerase activity was ~2.0-fold greater in prostate cancer cells when compared with BPH-1 cells (0.0587 ± 0.002 change in A_{475} nm per second per milligram of total protein, DU-145 and 0.0447 ± 0.004 change in A_{475} nm per second per milligram of total protein, LNCaP vs 0.0240 ± 0.003 change in A_{475} nm per second per milligram of total protein, BPH-1). MIF-associated tautomerase activity in cell lysates and spent culture medium was reduced in a dose-dependent manner by increasing concentrations of the MIF antagonist ISO-1 (Fig. 2, *A* and *B*). Although ISO-1 reduced MIF in vitro the tautomerase activity in the cell lysates and in the culture medium of all tested cell lines (Fig. 2, *A* and *B*), inactivation of bioactive MIF using ISO-1 preferentially decreased proliferation of DU-145 cells (Fig. 2*C*). Therefore, blockade of MIF's biological activity, either inside the cell or outside the cell

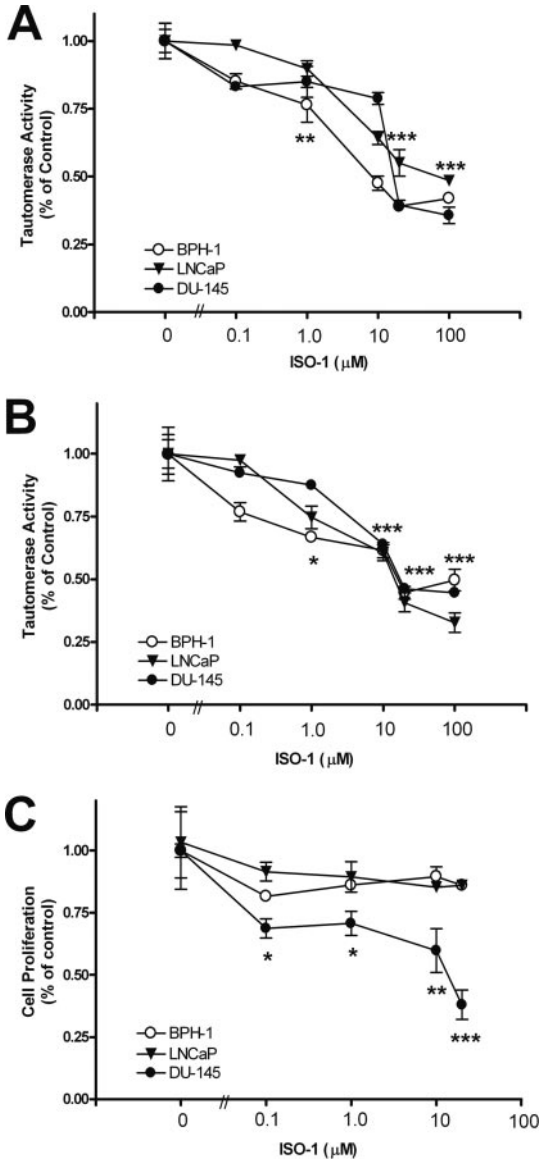

FIGURE 2. MIF tautomerase activity in BPH-1 and DU-145 cells. *A*, Bioactivity of MIF in cell lysates determined by in vitro tautomerase activity. MIF-associated tautomerase activity was determined using L-dopachrome methyl ester as a substrate. Cells were cultured to 80% confluency, and MIF tautomerase activity in the cell lysates was assayed by measuring the change in A_{475} nm over 2 min with the addition of increasing ISO-1. Data are expressed as change in A_{475} per second per microgram of total protein. Significant difference compared with DMSO control is represented by asterisks as follows: **, $p < 0.01$; ***, $p < 0.001$. Values represent the mean ± SEM of duplicate measurements in three experiments. *B*, Bioactivity of MIF secreted in cell culture medium determined by in vitro tautomerase activity. MIF-associated tautomerase activity was determined using L-dopachrome methyl ester as a substrate. Cells were cultured to 80% confluency, and MIF tautomerase activity in the cell culture medium was assayed by measuring the change in A_{475} nm over 2 min with the addition of increasing ISO-1. Data are expressed as change in A_{475} per second. Significant difference compared with DMSO control is represented by asterisks as follows: *, $p < 0.05$; ***, $p < 0.001$. Values represent the mean ± SEM of duplicate measurements in three experiments. *C*, Effect of MIF inhibitor, ISO-1, on prostate cell proliferation. Cells were cultured under standard conditions with the inclusion of increasing concentrations of ISO-1 for 18 h. Data are expressed as cell proliferation (percentage of control, DMSO) using 3 h of incubation with WST reagent at 37°C to assess relative cell numbers. Significant difference compared with DMSO control is represented by asterisks as follows: *, $p < 0.05$; **, $p < 0.01$; ***, $p < 0.001$. Values represent the mean ± SEM of duplicate measurements of three separate experiments.

(in the culture medium) resulted in decreased cell proliferation only in cells showing cell surface CD74 localization (DU-145), without affecting BPH-1 or androgen-dependent LNCaP cells.

Blocking MIF-CD74 interaction inhibits DU-145 cell proliferation, induces apoptosis, and reduces Matrigel invasion

Neutralizing Abs to MIF or CD74 inhibited the proliferation of DU-145 cells with anti-MIF showing a significant decrease within 24 h of treatment (Fig. 3*A*, $p < 0.05$) and anti-CD74 decreasing cell numbers at 48 h (Fig. 3*B*, $p < 0.01$). Anti-MIF or anti-CD74 treatments also induced apoptosis in DU-145 cells (Fig. 4*A*), indicating that cell viability in DU-145 cells is dependent upon functional MIF-CD74 interactions. These treatments had no effect on BPH-1 or LNCaP cells that lacked cell surface expression of CD74. Additionally, inclusion of anti-MIF or anti-CD74 with DU-145 cells in the upper Transwell chamber reduced Matrigel invasion (Fig. 5). Therefore, blocking MIF-CD74 interactions with neutralizing Abs specifically affected androgen-independent DU-145 cells.

Knockdown of MIF or CD74 expression by RNAi inhibits DU-145 cell proliferation and downstream MIF signaling

The effects of MIF or CD74 inactivation at the mRNA level were assessed by RNAi treatment. RNAi treatment decreased the associated mRNA and protein in all cell lines (Fig. 6 and data not shown). Unexpectedly, MIF RNAi treatment resulted in a dramatic

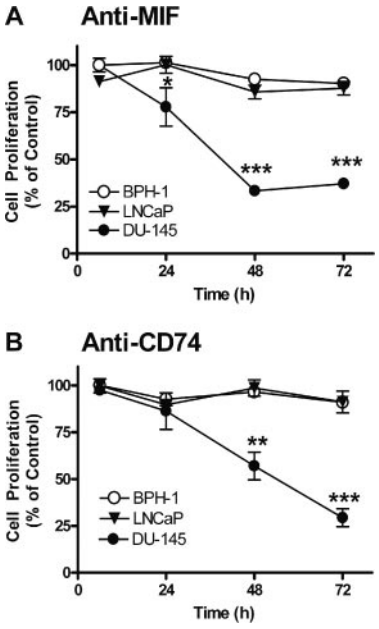

FIGURE 3. Effect of blocking MIF or its receptor (CD74) on prostate epithelial cell proliferation. *A*, Viability of BPH-1, LNCaP, and DU-145 cells treated with isotype control or anti-MIF Ab were determined by WST-1 assay. At each time point, 10 μl of WST-1 reagent (Pierce) was added to the culture medium and incubated at 37°C for 3 h. Percentage of control cells was calculated by dividing each treatment well A_{450} by mean isotype control well A_{450}. Data were determined from triplicate wells. Each point represents triplicate wells of mean percentage of WST-1 $A_{450} \pm$ SEM where significant difference compared with isotype control is represented by asterisks as follows: *, $p < 0.05$; ***, $p < 0.001$. Results are mean $\pm$ SEM of three separate experiments. *B*, Viability of BPH-1, LNCaP, and DU-145 cells treated with anti-CD74 Ab was determined by WST-1 assay as described above. Significant difference compared with isotype control is represented by asterisks as follows: **, $p < 0.01$; ***, $p < 0.001$. Results are mean $\pm$ SEM of three separate experiments.

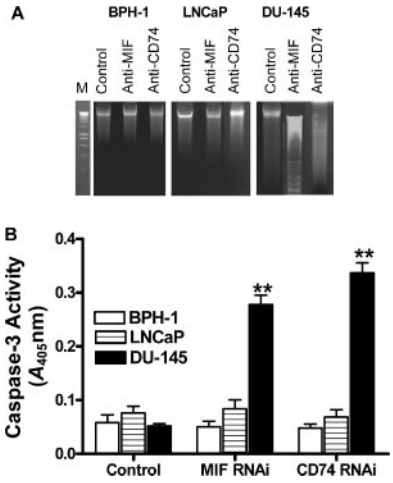

FIGURE 4. Blocking MIF or CD74 induces DU-145 cell apoptosis. *A*, DNA laddering was observed in DU-145 cells treated with anti-MIF or anti-CD74 (5 μg/ml) for 48 h. Two micrograms of genomic DNA from isotype control, anti-MIF or anti-CD74 Ab treated BPH-1, LNCaP, or DU-145 cells was run on 1.5% agarose gel stained with ethidium bromide and photographed under UV light. DNA markers were electrophoresed with a kilobase pair reference with band range from 10 to 0.5 kb (*lane M*). Figures depict representative samples from duplicate experiments displayed as composites of multiple gels. *B*, Caspase-3 activity was observed in DU-145 cells treated with MIF or CD74 RNAi. BPH-1, LNCaP, or DU-145 cells were preincubated with either scramble control, MIF, or CD74 RNAi for 48 h, washed and lysed, and total cellular protein was assayed for caspase-3-like activity by measuring the release of pNA from the colorimetric caspase-3 substrate z-DEVD-pNA. Treatment with MIF or CD74 RNAi increased constitutive caspase-3 activity in DU-145 cells. Each bar represents mean A_{405} nm $\pm$ SEM from triplicate wells. Significant difference compared with scramble control is indicated by asterisks as follows: **, $p < 0.01$. Results are mean $\pm$ SEM of two separate experiments.

increase in CD74 mRNA and protein by DU-145 cells (Fig. 6, *B* and *D*), suggesting a coordinated regulation of expression to result in receptor up-regulation when the agonist amounts are depressed. As was seen with ISO-1 and neutralizing Ab treatment, MIF or CD74 RNAi treatment only affected proliferation of DU-145 cells (Fig. 6*E*). Reduction in MIF or CD74 mRNA and the associated decrease in detectable protein did not affect BPH-1 or LNCaP cell proliferation (data not shown). MIF or CD74 RNAi induced apoptosis only in DU-145 cells (Fig. 4*B*).

The role of MIF-CD74 interaction in the activation of prostate cancer cell downstream signaling pathways is not known. We examined the effect of decreasing available MIF on measurable changes in MIF signal transduction by analyzing phosphorylated ERK (p-ERK) 1/2 amounts in BPH-1 and DU-145 cells treated by MIF or CD74 RNAi. MIF or CD74 RNAi reduced p-ERK 1/2 amounts in DU-145 cells when normalized to total ERK 1/2 protein (Fig. 7*A*, $p < 0.001$); neither MIF RNAi nor CD74 RNAi treatment had an effect on BPH-1 or LNCaP cells' p-ERK 1/2 amounts (Fig. 7*B*).

To extend the previous findings, RNAi-induced changes in DU-145 gene expression were determined by targeted array analysis using a human cancer (HS-044) and a G-protein receptor (HS-025) array, each containing sequences for 96 different genes. Of the 192 genes examined, a total of 18 were affected by either MIF and/or CD74 RNAi. Expression of eight genes (bcl-2, lysophosphatidic acid G-protein receptor (EDG-7), early growth response-1 (EGR-1), glutamate receptor-4 (GRM-4), IL-1β, IL-6, jun (AP-1), TNF-α were down-regulated at least 2.5-fold by both MIF RNAi and CD74 RNAi (Table I). While expression of two genes

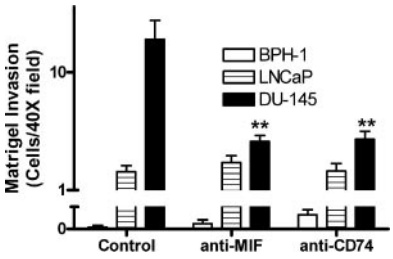

FIGURE 5. Blocking MIF or CD74 reduces in vitro invasion of DU-145 cells. Comparison of invading BPH-1, LNCaP, or DU-145 cells with MIF or CD74 Ab treatment. Invasion assays were performed in 24-well Transwell chambers containing Matrigel-coated polycarbonate filters with 12 μm pores. Invading cells in nine representative fields were counted under a microscope at $\times$400 magnification. Each bar represents the mean number of invading cells $\pm$ SEM from triplicate filters of two separate experiments. Significant difference compared with isotype control is indicated by asterisks as follows: **, $p < 0.01$.

(GRM-8 and opioid receptor κ 1 (OPR-κ 1)) were up-regulated at least 2.5-fold by MIF RNAi and CD74 RNAi (Table I). MIF RNAi specifically down-regulated the expression of cyclin D1 (5.2-fold, CCN-D1) and cyclooxygenase-2 (6.9-fold, COX-2), but up-regulated the expression of p27 (3.5-fold, CDKN-1B). CD74 RNAi specifically down-regulated the expression of cyclin E2 (3.9-fold, CCN-E2), but specifically up-regulated the expression of type 1 collagen (2.8-fold, COL1-α1), heat shock protein 90 kDa (3.7-fold, HSPCA), prolactin (2.6-fold, PRL) and prostaglandin E receptor (4.2-fold, PTGER-1). Although all of these genes are known to be expressed in the prostate, these results are the first to document a requirement for MIF and/or CD74 expression in the regulation of the aforementioned genes. The gene expression changes in Bcl-2, cyclin D1, and cyclin E2 detected by arrays were verified by Western blot analysis. MIF RNAi resulted in decreased protein amounts of both Bcl-2 and cyclin D1, whereas CD74 RNAi treatment resulted in decreased amounts of Bcl-2, cyclin D1, and cyclin E2 (Fig. 8).

Effects of in vivo treatment with ISO-1 on tumor angiogenesis and growth in DU-145 xenografts

We examined whether blocking MIF using the antagonist ISO-1 could inhibit the in vivo growth and neovascularization of androgen-independent DU-145 prostate tumors. The dose of ISO-1 used in this study was based on a previous report (31). The mean tumor volume after 35 days of treatment was significantly smaller in the ISO-1 treated animals (300.3 $\pm$ 58.6 mm^3) compared with the controls (776.8 $\pm$ 82.6 mm^3; Fig. 9*A*; $p < 0.01$). In addition, total tumor weight after treatment in the ISO-1-treated animals was significantly smaller than in the control mice ($p < 0.05$; Fig. 9*B*). Serum MIF and total tumor MIF amounts were determined using a human MIF ELISA, which we previously determined does not detect mouse MIF (7, 8). ISO-1 treatment did not change the total tumor human MIF per protein content (491.9 $\pm$ 80.2 vs 421.2 $\pm$ 40.6 ng/mg in control and treated, respectively), but ISO-1 treatment did significantly reduce total human serum MIF (1.54 ng/ml controls, 0.89 ng/ml with ISO-1 treatment; $p < 0.05$), indicating that ISO-1 treatment may have decreased tumor-secreted MIF.

Tumor cell growth and viability was assessed by PCNA staining, which demonstrated that ISO-1 treatment significantly decreased the number of proliferating cells (21.88 $\pm$ 12.06 cells per field) within the solid tumors compared with controls (192.6 $\pm$ 11.24 cells per field; Fig. 9*C*; $p < 0.001$). Neovascularization was assessed by CD34 immunostaining of vascular epithelial cells and counting microvessels in tumors. Mean microvessel staining in the ISO-1 treatment group was 5.67 $\pm$ 1.45 microvessels, which was significantly lower than that in the control group (31.33 $\pm$ 8.69 microvessels; Fig. 9*D*; $p < 0.05$). Mean animal body weights, as well as overall activity, were similar in both groups at the completion of the experiment, suggesting that ISO-1 had no major side effects on these mice (data not shown).

Discussion

MIF is a constitutively expressed, multifunctional cytokine that plays a key regulatory role in inflammation and in both innate and adaptive immune responses (9, 32). MIF functions to counterregulate the effects of glucocorticoids and to stimulate the synthesis and secretion of other proinflammatory mediators such as TNF-α and IL-1β, and as such, it has been suggested that MIF is a key initiator of the inflammatory cascade (30, 32, 33). In addition, MIF is an autocrine regulator of cell proliferation and differentiation. Serum-starved NIH/3T3 cells secreted endogenous MIF as a consequence of serum stimulation resulting in proliferation of quiescent cells. This response was associated with phosphorylation and subsequent activation of ERK 1/2 (34, 35). Inability to modulate the MIF autocrine loop may result in localized chronic inflammation, and the resultant epithelial cell injury may play a role in carcinogenesis. Our current results suggest that cell surface expression of

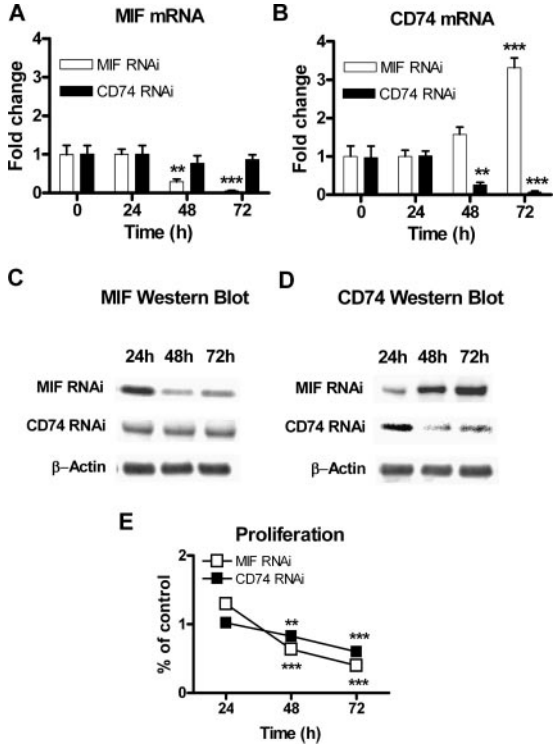

FIGURE 6. Effect of RNAi on MIF and CD74 expression and cell proliferation in DU-145 cells. DU-145 cells were treated with RNAi with samples taken at 24-h intervals. Gene expression was assessed by real-time RT-PCR. Total cell lysates were used to determine MIF and CD74 protein amounts by Western blots. Cell proliferation was assessed by WST-1 assay with each point representing mean percentage of WST-1 A_{450} $\pm$ SEM of triplicate wells. Significant difference compared with RNAi scramble control is represented by asterisks as follows: **, $p < 0.01$; ***, $p < 0.001$. All results are representative of three separate experiments. *A*, MIF mRNA amounts in RNAi-treated DU-145 cells. *B*, CD74 mRNA amounts in RNAi-treated DU-145 cells. *C*, Total MIF protein detected by Western blot in MIF or CD74 RNAi-treated DU-145 cell lysates. *D*, Total CD74 protein detected by Western blot in MIF or CD74 RNAi-treated DU-145 cell lysates. *E*, Cell proliferation in RNAi-treated DU-145 cells.

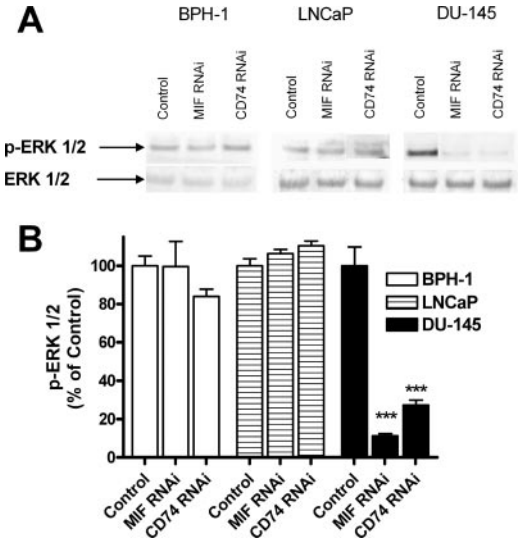

FIGURE 7. p-ERK 1/2 amounts in BPH-1, LNCaP, or DU-145 cells treated with MIF or CD74 RNAi. *A*, ERK 1/2 Western blots. ERK 1/2 activation was examined by blotting with p-ERK 1/2 Ab (AF-1018; R&D Systems). The stripped membrane was reprobed with total ERK 1/2 Ab (AF-1576; R&D Systems). Figures depict representative samples from triplicate experiments displayed as composites of multiple gels. *B*, p-ERK 1/2 was quantified by determining total p-ERK 1/2 band intensity and dividing by total ERK 1/2 band intensity for each sample. Data are expressed as percentage of control p-ERK 1/2 for each cell line. Values represent the mean value ± SEM of duplicate measurements of triplicate experiments. Significant difference compared with RNAi scramble control is represented by asterisks as follows: ***, $p < 0.001$.

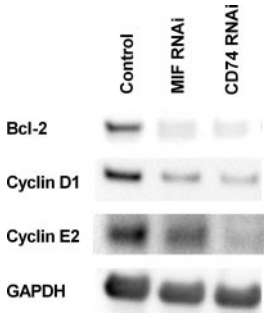

FIGURE 8. Western blots of DU-145 RNAi-treated cell lysates. Changes in gene expression detected in arrays were verified by Western blotting of RNAi-treated DU-145 cell lysates. Figures depict representative samples from duplicate experiments.

CD74 is a key step in MIF-mediated signal transduction and may play an important role in androgen-independent prostate cancer.

It is difficult to account for the absence of a MIF response under "normal" physiological conditions, considering the ubiquitous expression of this protein. All prostate epithelial cell lines examined release MIF into the culture medium (data not shown), suggesting that bioactive MIF is readily available in the local environment. In addition, increased MIF-CD74 and MIF-CD44v9 complex formation was observed in prostate cancer cells. However, cell surface expression of CD74 was only observed in androgen-independent (DU-145) prostate cancer cells. This is an intriguing and novel observation, but whether this finding applies to other androgen-independent prostate cancer cells remains to be determined. CD44v9, although increased in prostate cancer cells (36), was not increased at the cell surface. Taken together, these data suggest that although CD44 may be necessary for CD74 signaling (21, 22), it is not a regulating mechanism because it is present in overabundance and in steady-state levels at the cell surface. Therefore, these results suggest that up-regulation of cell surface CD74 is the necessary step in mediating MIF-CD74-activated signal transduction. Thus, blocking MIF-CD74 interactions (presumably at the cell surface) either by pharmacologic inhibition of MIF (e.g., ISO-1) or decreasing MIF and/or CD74 would have little effect on normal cell function (indicating that these cells are not dependent on MIF-mediated signal transduction) but may provide a potent inhibition of cancer cell proliferation (indicating that these cells are dependent on MIF-mediated signal transduction). Therefore, it is possible that in normal prostate epithelial cells, MIF may be important for optimal cell growth under certain specific conditions (e.g., inflammation), whereas in cancer cells, there is a reliance upon MIF-dependent ERK activation to sustain cell proliferation resulting in increased MIF and CD74 expression. In fact, our present findings confirm this hypothesis because blocking MIF protein (anti-MIF), message (RNAi), and/or activity (ISO-1) had little or no effect on benign BPH-1 cells or androgen-dependent LNCaP cells but resulted in decreased DU-145 cell proliferation and viability.

TABLE 1. *Array analysis of gene expression that is altered in DU-145 prostate cancer cells by MIF or CD74 RNAi*

RefSeq	Gene Symbol	Common Name	MIF RNAi	CD74 RNAi
NM_000633	BCL-2	Bcl-2	−3.4	−3.7
NM_004064	CDKN1B	p27(KIP1)	3.5	NA
NM_053056	CCND1	Cyclin D1	−5.2	NA
NM_004702	CCNE2	Cyclin E2	NA	−3.9
NM_000088	COL1A1	Collagen, type I, α1	NA	2.8
NM_012152	EDG-7	Lysophosphatidic acid G-protein-coupled receptor 7	−2.9	−3.4
NM_001964	EGR-1	Early growth response 1	−3.7	−4.2
NM_000841	GRM-4	Glutamate receptor, metabotropic 4	−2.9	−3.3
NM_000845	GRM-8	Glutamate receptor, metabotropic 8	4.6	4.1
NM_005348	HSPCA	Heat shock protein 90 kDa α	NA	3.7
NM_000576	IL-1β	IL-1β	−5.3	−6.9
NM_000600	IL-6	IL-6	−4.9	−3.9
NM_002228	Jun	AP-1	−4.8	−3.9
NM_000912	OPRκ1	Opioid receptor κ1	3.4	2.9
NM_000948	PRL	Prolactin	NA	2.6
NM_000955	PTGER1	Prostaglandin E receptor 1	NA	4.2
NM_000963	PTGS2	Cyclooxygenase 2	−6.9	NA
NM_000594	TNF-α	Tumor necrosis factor α	−15.0	−5.5

NA, Not applicable.

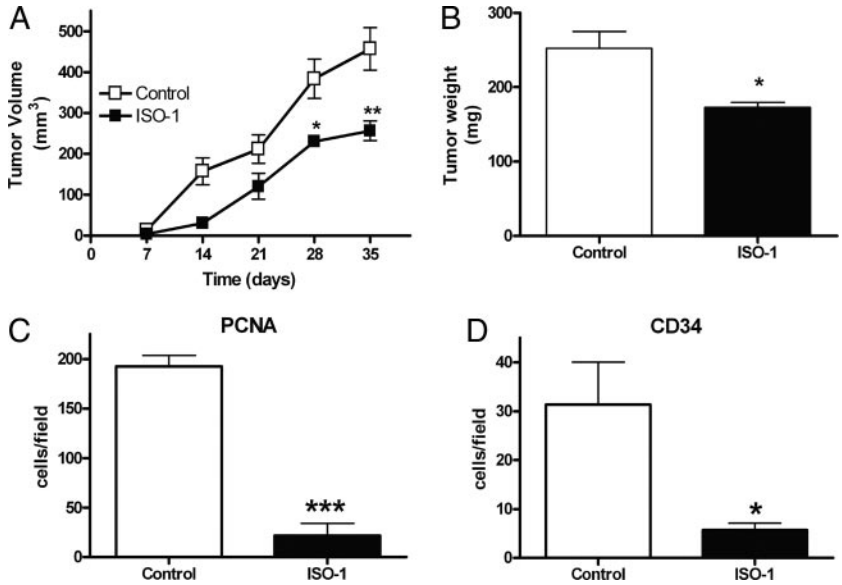

FIGURE 9. Effects of in vivo ISO-1 treatment on DU-145 tumor growth and angiogenesis. *A*, Tumor volumes were measured at weekly intervals. Points represent mean tumor volume ± SEM. Significant difference compared with DMSO control is represented by asterisks as follows: *, $p < 0.05$; **, $p < 0.01$. *B*, Weights of excised tumors (mg) were determined at the end of 35 days of ISO-1 treatment. Bars represent mean tumor weight ± SEM ($n = 4$). Significant difference compared with DMSO control is represented by asterisks as follows: *, $p < 0.05$. *C*, Tumor cell viability was assessed by PCNA staining. The total number of cells per field was determined from ten fields of triplicate sections from each tumor. Bars represent mean positive staining nuclei ± SEM ($n = 4$). Significant difference compared with DMSO control is represented by asterisks as follows: ***, $p < 0.001$. *D*, Effects of ISO-1 treatment on angiogenesis was determined by microvessel counting determined by CD34 immunostaining of excised xenograft tumors. Bars represent mean positive staining cells ± SEM ($n = 4$). Significant difference compared with DMSO control is represented by asterisks as follows: *, $p < 0.05$.

Numerous studies have determined that reducing tumor MIF results in decreased cell proliferation (11), induction of apoptosis (13) and reduction in the synthesis and secretion of other growth factors (23, 37, 38). In accordance with these findings, the treatments used in the present study were found to suppress DU-145 cell proliferation and induce apoptosis. The molecular mechanism(s) associated with MIF function in the prostate are not fully understood. However, because DU-145 cells appear to have abundant (compared with other prostate cells examined in this study) cell surface localization of CD74, it would be expected that alteration of MIF and/or CD74 should also affect the expression and secretion of other proinflammatory molecules. Interestingly, our results show decreased expression of IL-1β, TNF-α, and IL-6, with either MIF or CD74 RNAi treatment lending evidence for MIF, through binding with cell surface CD74, as a modulator of cytokine production in prostate cancer cells.

MIF-CD74 interaction activates the ERK 1/2 signaling pathway, presumably through interaction with CD44 (21). Interestingly, there is no information as to the other pathways and/or signaling molecules (aside from ERK activation) that are affected by MIF-CD74 interaction, although a recent report suggests that MIF engagement of CD74 augments B cell survival by increasing the expression of Bcl-x_L (20). We determined whether MIF and/or CD74 deficiency influenced downstream targets of MAPK using targeted array analysis. The results presented in this study document significant changes in the expression of known MIF downstream signaling molecules that affect prostate cancer cell viability and emergence of androgen-independent cell growth, such as cyclin D1 (39), p27 (40), and bcl-2 (41). Cyclin D1 is a critical regulator involved in cell cycle progression through the G_1 phase into the S phase, thereby controlling cell proliferation, and its expression is attributed to ERK 1/2 activation (42). Our studies document that inhibition of the MIF and/or CD74 decreases cyclin D1 gene expression. A number of studies have shown that the induction of cyclin D1 expression requires activation of the MAPK pathway and that cyclin D1 expression is temporally preceded by the activation of a class of genes known as immediate-early genes, such as jun (AP-1) and Egr-1 (42, 43). The present study documents that inhibition of MIF and/or CD74 also results in decreased expression of jun and Egr-1, suggesting that MIF-CD74 interaction resulting in ERK 1/2 activation is a key initiator of DU-145 cyclin D1-regulated cell proliferation.

Based upon data obtained in the present study, we suggest that cell surface expression of CD74 is the rate-limiting member of the MIF-signal transduction complex. In DU-145 cells, large quantities of MIF are constitutively synthesized and secreted. The MIF-CD74 complex (in association with CD44v9) activates MAPK signal transduction pathways resulting in up-regulation of cyclin D1 and sustained cell proliferation.

In the DU-145 xenograft model, ISO-1 treatment suppressed angiogenesis and in vivo tumor growth. This is the first report of the inhibitory effects of ISO-1 treatment on in vivo tumor growth. Our results, therefore, support the hypothesis that the therapeutic effect of blocking MIF on tumor growth is attributable in part to the inhibition of angiogenesis.

In summary, the present study shows increased MIF and CD74 expression in the aggressive androgen-independent DU-145 prostate cancer cell line. In addition, this cell line had significant amounts of cell surface CD74, an event that was not observed for benign or androgen-dependent cell lines. Blocking MIF-CD74 interaction selectively decreased ERK 1/2 activation, decreased cell proliferation, and increased apoptosis in DU-145 cells only, while being ineffective in benign cells (BPH-1) or androgen-dependent cells (LNCaP). The emerging role of MIF and its receptor (CD74) in prostate tumorigenesis suggest that modulating this cytokine's activity may result in new, selective, therapeutic modalities for men with androgen-independent prostate cancer.

Acknowledgments

Gary A. Smith, Jr. and Michael A. Bellino provided technical assistance. We thank Irving Nadelhaft for the use of this microscope/digital camera system.

Disclosures

The authors have no financial conflict of interest.

References

1. Cordon-Cardo, C., and C. Prives. 1999. At the crossroads of inflammation and tumorigenesis. *J. Exp. Med.* 190: 1367–1370.
2. Coussens, L. M., and Z. Werb. 2002. Inflammation and cancer. *Nature* 420: 860–867.
3. Platz, E. A., and A. M. DeMarzo. 2004. Epidemiology of inflammation and prostate cancer. *J. Urol.* 171: S36–S40.
4. Taylor, M. L., A. Mainous, G. 3rd, and B. J. Wells. 2005. Prostate cancer and sexually transmitted diseases: a meta-analysis. *Fam. Med.* 37: 506–512.
5. Dennis, L. K., and D. V. Dawson. 2002. Meta-analysis of measures of sexual activity and prostate cancer. *Epidemiology* 13: 72–79.
6. Kawakami, J., D. R. Siemens, and J. C. Nickel. 2004. Prostatitis and prostate cancer: implications for prostate cancer screening. *Urology* 64: 1075–1080.
7. Meyer-Siegler, K. L., M. A. Bellino, and M. Tannenbaum. 2002. Macrophage migration inhibitory factor evaluation compared with prostate specific antigen as a biomarker in patients with prostate carcinoma. *Cancer* 94: 1449–1556.
8. Meyer-Siegler, K. L., K. A. Iczkowski, and P. L. Vera. 2005. Further evidence for increased macrophage migration inhibitory factor expression in prostate cancer. *BMC Cancer* 5: 73.
9. Baugh, J. A., and R. Bucala. 2002. Macrophage migration inhibitory factor. *Crit. Care Med.* 30: S27–S35.
10. Baugh, J. A., and S. C. Donnelly. 2003. Macrophage migration inhibitory factor: a neuroendocrine modulator of chronic inflammation. *J. Endocrinol.* 179: 15–23.
11. Mitchell, R. A., and R. Bucala. 2000. Tumor growth-promoting properties of macrophage migration inhibitory factor (MIF). *Semin. Cancer Biol.* 10: 359–366.
12. Mitchell, R. A., H. Liao, J. Chesney, G. Fingerle-Rowson, J. Baugh, J. David, and R. Bucala. 2002. Macrophage migration inhibitory factor (MIF) sustains macrophage proinflammatory function by inhibiting p53: regulatory role in the innate immune response. *Proc. Natl. Acad. Sci. USA* 99: 345–350.
13. Hudson, J. D., M. A. Shoaibi, R. Maestro, A. Carnero, G. J. Hannon, and D. H. Beach. 1999. A proinflammatory cytokine inhibits p53 tumor suppressor activity. *J. Exp. Med.* 190: 1375–1382.
14. Henne, C., F. Schwenk, N. Koch, and P. Moller. 1995. Surface expression of the invariant chain (CD74) is independent of concomitant expression of major histocompatibility complex class II antigens. *Immunology* 84: 177–182.
15. Busch, R., C. H. Rinderknecht, S. Roh, A. W. Lee, J. J. Harding, T. Burster, T. M. Hornell, and F. D. Mellins. 2005. Achieving stability through editing and chaperoning: regulation of MHC class II peptide binding and expression. *Immunol. Rev.* 207: 242–260.
16. Wilson, K. M., M. O. Labeta, G. Pawelec, and N. Fernandez. 1993. Cell-surface expression of human histocompatibility leucocyte antigen (HLA) class II-associated invariant chain (CD74) does not always correlate with cell-surface expression of HLA class II molecules. *Immunology* 79: 331–335.
17. Meyer-Siegler, K. L., and P. L. Vera. 2005. Substance P induced changes in CD74 and CD44 in the rat bladder. *J. Urol.* 173: 615–620.
18. Ong, G. L., D. M. Goldenberg, H. J. Hansen, and Mattes, M. J. 1999. Cell surface expression and metabolism of major histocompatibility complex class II invariant chain (CD74) by diverse cell lines. *Immunology* 98: 296–302.
19. Leng, L., C. N. Metz, Y. Fang, J. Xu, S. Donnelly, J. Baugh, T. Delohery, Y. Chen, R. A. Mitchell, and Bucala, R. 2003. MIF signal transduction initiated by binding to CD74. *J. Exp. Med.* 197: 1467–1476.
20. Starlets, D., Y. Gore, I. Binsky, M. Haran, N. Harpaz, L. Shvidel, S. Becker-Herman, A. Berrebi, and I. Shachar. 2006. Cell surface CD74 initiates a signaling cascade leading to cell proliferation and survival. *Blood* 107: 4807–4816.
21. Naujokas, M. F., M. Morin, M. S. Anderson, M. Peterson, and J. Miller. 1993. The chondroitin sulfate form of invariant chain can enhance stimulation of T cell responses through interaction with CD44. *Cell* 74: 257–268.
22. Naujokas, M. F., L. S. Arneson, B. Fineschi, M. E. Peterson, S. Sitterding, A. T. Hammond, C. Reilly, D. Lo, and J. Miller. 1995. Potent effects of low levels of MHC class II-associated invariant chain on $CD4^+$ T cell development. *Immunity* 3: 359–372.
23. Meyer-Siegler, K. L., E. C. Leifheit, and P. L. Vera. 2004. Inhibition of macrophage migration inhibitory factor decreases proliferation and cytokine expression in bladder cancer cells. *BMC Cancer* 4: 34.
24. Iczkowski, K. A., C.G. Pantazis, and J. Collins. 1997. The loss of expression of CD44 standard and variant isoforms is related to prostatic carcinoma development and tumor progression. *J. Urol. Pathol.* 6: 119–129.
25. Agus, D. B., C. Cordon-Cardo, W. Fox, M. Drobnjak, A. Koff, D.W. Golde, and H. I. Scher. 1999. Prostate cancer cell cycle regulators: response to androgen withdrawal and development of androgen independence. *J. Natl. Cancer Inst.* 91: 1869–1876.
26. Zhong, X. B., Leng, L., Beitin, A., Chen, R., McDonald, C., Hsiao, B., Jenison, R. D., Kang, I., Park, S. H., Lee, et al. 2005. Simultaneous detection of microsatellite repeats and SNPs in the macrophage migration inhibitory factor (MIF) gene by thin-film biosensor chips and application to rural field studies. *Nucleic Acids Res.* 33: 121–129.
27. Bernhagen, J., Mitchell, R. A., Calandra, T., Voelter, W., Cerami, A., and Bucala, R. 1994. Purification, bioactivity, and secondary structure analysis of mouse and human macrophage migration inhibitory factor MIF. *Biochemistry* 33: 14144–14155.
28. Dios, A., R. A. Mitchell, B. Aljabari, J. Lubetsky, K. O'Connor, H. Liao, P. D. Senter, K. R. Manogue, E. Lolis, C. Metz, et al. 2002. Inhibition of MIF bioactivity by rational design of pharmacological inhibitors of MIF tautomerase activity. *J. Med. Chem.* 45: 2410–2416.
29. Livak, K. J., and T. D. Schmittgen. 2001. Analysis of relative gene expression data using real-time quantitative PCR and the $2(-\Delta\Delta C_T)$ *Methods.* 24: 402–408.
30. Lue, H., R. Kleemann, T. Calandra, T. Roger, and J. Bernhagen. 2002. Macrophage migration inhibitory factor (MIF): mechanisms of action and role in disease. *Microbes Infect.* 4: 449–460.
31. Al-Abed, Y., D. Dabideen, B. Aljabari, A. Valster, D. Messmer, M. Ochani, M. Tanovic, K. Ochani, M. Bacher, F. Nicoletti, et al. 2005. ISO-1 binding to the tautomerase active site of MIF inhibits its pro-inflammatory activity and increases survival in severe sepsis *J. Biol. Chem.* 280: 36541–36544.
32. Fingerle-Rowson, G., P. Koch, R. Bikoff, X. Lin, C. N. Metz, F. S. Dhabhar, A. Meinhardt, and R. Bucala. 2003. Regulation of macrophage migration inhibitory factor expression by glucocorticoids in vivo. *Am. J. Pathol.* 162: 47–56.
33. Calandra, T., J. Bernhagen, C. N. Metz, L. A. Spiegel, M. Bacher, T. Donnelly, A. Cerami, and R. Bucala. 1995. MIF as a glucocorticoid-induced modulator of cytokine production. *Nature* 377: 68–71.
34. Roger, T., A. L., Chanson, M. Knaup-Reymond, and T. Calandra. 2005. Macrophage migration inhibitory factor promotes innate immune responses by suppressing glucocorticoid-induced expression of mitogen-activated protein kinase phosphatase-1. *Eur. J. Immunol.* 35: 3405–3413.
35. Mitchell, R. A., C. N. Metz, T. Peng, and R. Bucala. 1999. Sustained mitogen-activated protein kinase (MAPK) and cytoplasmic phospholipase A2 activation by macrophage migration inhibitory factor (MIF). Regulatory role in cell proliferation and glucocorticoid action. *J. Biol. Chem.* 274: 18100–18106.
36. Iczkowski, K. A., S. Bai, and C. G. Pantazis. 2003. Prostate cancer overexpresses CD44 variants 7–9 at the messenger RNA and protein level. *Anticancer Res.* 23: 3129–3140.
37. Ren, Y., H. T. Tsui, R. T. Poon, I. O. Ng, Z. Li, Y. Chen, G. Jiang, C. Lau, W. C. Yu, M. Bacher, and S. T. Fan. 2003. Macrophage migration inhibitory factor: roles in regulating tumor cell migration and expression of angiogenic factors in hepatocellular carcinoma. *Int. J. Cancer* 107: 22–29.
38. Shimizu, T., R. Abe, H. Nakamura, A. Ohkawara, M. Suzuki, and J. Nishihira. 1999. High expression of macrophage migration inhibitory factor in human melanoma cells and its role in tumor cell growth and angiogenesis. *Biochem. Biophys. Res. Commun.* 264: 751–758.
39. Swant, J. D., B. E. Rendon, M. Symons, and R. A Mitchell. 2005. Rho GTPase-dependent signaling is required for MIF-mediated expression of cyclin D1. *J. Biol. Chem.* 280: 23066–23072.
40. Kleemann, R., A. Hausser, G. Geiger, R. Mischke, A. Burger-Kentischer, O. Flieger, F. J. Johannes, T. Roger, T. Calandra, A. Kapurniotu, et al. 2000. Intracellular action of the cytokine MIF to modulate AP-1 activity and the cell cycle through Jab1. *Nature* 408: 211–216.
41. Baumann, R., C. Casaulta, D. Simon, S. Conus, S. Yousefi, and H. U. Simon. 2003. Macrophage migration inhibitory factor delays apoptosis in neutrophils by inhibiting the mitochondria-dependent death pathway. *FASEB J.* 17: 2221–2230.
42. Xiao, D., D. Chinnappan, R. Pestell, C. Albanese, and H. C. Weber. 2005. Bombesin regulates cyclin D1 expression through the early growth response protein Egr-1 in prostate cancer cells. *Cancer Res.* 65: 9934–9942.
43. Shiozawa, T., T. Miyamoto, H. Kashima, K. Nakayama, T. Nikaido, and I. Konishi. 2004. Estrogen-induced proliferation of normal endometrial glandular cells is initiated by transcriptional activation of cyclin D1 via binding of c-Jun to an AP-1 sequence. *Oncogene* 23: 8603–8610.